Lithospheric studies using gradients from close encounters of Ørsted, CHAMP, and SAC-C

Michael E. Purucker[1]

[1]*Raytheon at Planetary Geodynamics Lab, GSFC/NASA, USA*

(Received ; Revised ; Accepted)

Maps of the lithospheric magnetic field made to date have used single satellite observations. In contrast, the upcoming *Swarm* mission will measure the magnetic field gradient, in this case the difference in the magnetic field between the lower two satellites. We discuss the optimum satellite separation, and the expected resolution achievable. We relate this gradient to underlying magnetic field sources. In an attempt to better understand the advantages and limitations of gradient measurements, we have reviewed the Ørsted, SAC-C, and CHAMP missions for close encounters, and examined some $50,000$ of those observations in detail. The lithospheric signal over the north polar cap is reliably isolated by standard selection criteria, with about 20% of the data retained. We demonstrate that, at least in the polar caps, the selection criteria are necessary for the isolation of the lithospheric signal. There is a tendency for the predictions to underestimate the observed field, as shown by the slopes, which average about 2. This is especially notable over stronger anomalies. These gradients have evidently captured unmodeled, probably higher frequency, signal. Comparing the gradient measurement with the field measurement, we see a notable improvment in both the correlation coefficient and the offset, with the correlation coefficient improving from about 0.7 to in excess of 0.8. The gradient control provided by SAC-C and Ørsted is almost equally effective.

Key words: gradient, magnetic field, satellite, lithosphere

1. Introduction

The lithospheric magnetic anomaly field is produced by variations in the magnetization carried by crustal and some mantle rocks. Satellite maps of the lithospheric magnetic field made to date have used single satellite observations. In contrast, the upcoming *Swarm* mission will measure the magnetic field gradient, in this case the vector difference in the magnetic field between the lower two satellites which will fly side by side about 150 km apart. Near the geomagnetic pole, airborne surveys of the magnetic field gradient are used in place of measurements of the total field in order to reduce the influence of the rapidly time-varying external field [*Hood and Teskey*, 1989]. A gradient measurement enhances the shorter wavelength components of the signal, and as a consequence filters out much of the core and long wavelength external field. A corollary is that a gradient measurement also enhances the noise. Gradient measurements have found utility in determining the orientation of lineated magnetic anomalies [*Parker*, 1997; *Harrison and Southam*, 1991]. An annotated bibliography on magnetic field gradiometry, compiled by B. Huang and including unpublished reports, is available at http://planetary-mag.net/gradiometry.

In this paper, we demonstrate the enhanced resolution and increased accuracy possible when using the gradient of the magnetic field, as opposed to the field itself. We discuss our rationale for choosing the satellite separation, and the expected resolution achievable. We relate this gradient to the underlying magnetic field sources, and illustrate its utility with close encounter total field data from CHAMP, Ørsted, and SAC-C.

2. Gradients and close encounter data from Swarm

To improve the resolution of lithospheric magnetization mapping, the two lower *Swarm* satellites will fly at altitudes of about 400 km. The selected altitude ranges will, however, be compatible with a multi-year mission lifetime. Further improvement in the retrieval of the high-degree magnetic anomalies field can be achieved by considering gradients in the inversion algorithm, in addition to the full magnetic field readings. This concept for emphasising the small-scale anomalies by partially counteracting the attenuation effect with altitude has already been accepted and applied in gravity missions like GRACE and GOCE [*ESA*, 1999]. Optimal spacecraft separations for deriving the gradients are dependent on signal spectrum and instrument resolution.

Table 1. Statistics summarizing close encounters poleward of 60° North.

Satellite(s)	Cor. Coeff.	slope	offset (nT)	Number	Kp	Local Time	Along track gradient (nT, betw. adj. obs.)	Min. Max. (nT)	Notes
CHAMP - Ørsted	0.84	2.0	2.0	546	1^+, 2^0	Night	< 0.3	-10/+17	Fig. 3 (top)
CHAMP alone	0.71	2.7	-6.4	546	1^+, 2^0	Night	< 0.3	-13/+21	
CHAMP - SAC-C	0.83	2.0	-0.3	283	1^+, 2^0	Night	< 0.3	-5/+14	Fig. 3 (bottom)
CHAMP alone	0.68	2.1	-9.8	283	1^+, 2^0	Night	< 0.3	-9/+19	
CHAMP - SAC-C	0.23	large	0.2	2794	None	All	None	-10/+20	No selection
CHAMP - SAC-C	0.32	20	-0.9	1457	None	Night	None	-10/+19	
CHAMP - SAC-C	0.58	2.6	0.5	367	1^+, 2^0	Night	None	-9/+19	
CHAMP - Ørsted	-0.06	large	0.1	5889	None	All	None	-10/+18	No selection
CHAMP - Ørsted	0.25	15	-0.3	3304	None	Night	None	-10/+17	
CHAMP - Ørsted	0.81	2.1	2.5	738	1^+, 2^0	Night	None	-10/+17	

Table 2. Statistics summarizing close encounters poleward of 60° South.

Satellite(s)	Cor. Coeff.	slope	offset (nT)	Number	Kp	Local Time	Along track gradient (nT, betw. adj. obs.)	Min. Max. (nT)
CHAMP - Ørsted	0.28	8	0.2	1027	1^+, 2^0	Night	< 0.3	-5/+5
CHAMP alone	0.1	large	-0.4	1027	1^+, 2^0	Night	< 0.3	-6/+7
CHAMP - SAC-C	0.48	2.5	1.3	309	1^+, 2^0	Night	< 0.3	-10/+4
CHAMP alone	0.53	5	-2.8	309	1^+, 2^0	Night	< 0.3	-5/+15

Table 3. Statistics summarizing mid-latitude close encounters

Satellite(s)	Cor. Coeff.	slope	offset (nT)	Number	Kp	Local Time	Along track gradient (nT, betw. adj. obs.)	Min. Max. (nT)
CHAMP - Ørsted	0.60	2.4	0.2	321	1^+, 2^0	Night	< 0.3	-4/+2
CHAMP alone	-0.56	large	-1.0	321	1^+, 2^0	Night	< 0.3	-6/+4
CHAMP - SAC-C	0.69	1.8	0.3	647	1^+, 2^0	Night	< 0.3	-4/+8
CHAMP alone	0.39	9	-0.5	647	1^+, 2^0	Night	< 0.3	-6/+10

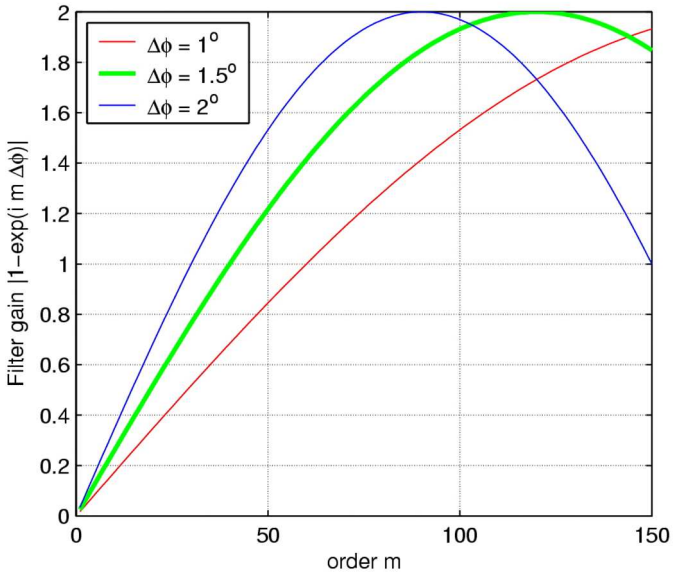

Fig. 1. Relative sensitivity of the gradient method versus spatial scales (spherical harmonic order m). Three examples with different spacecraft separations in longitude are shown.

2.1 Optimal separation

In order to find the optimal longitudinal separation of the lower pair of satellites for crustal field studies, we consider the following scenario: The scalar potential describing the crustal field $\mathbf{B}_{\rm cr} = -\mathrm{Re}\{\mathrm{grad}\, V\}$, is given as a spherical harmonic expansion,

$$V_{\rm cr} = a \sum_{n=1}^{n_{\max}} \sum_{m=0} \left(\frac{a}{r}\right)^{n+1} \gamma_n^m P_n^m e^{im\phi}.$$

This is the complex form of the usual spherical harmonic summation used in geomagnetism, with $\gamma_n^m = g_n^m - ih_n^m$.

The difference of the magnetic field measured by two satellites flying simultaneously with a longitudinal separation $\Delta\phi$ is $\Delta\mathbf{B}_{\rm cr} = \mathbf{B}_{\rm cr}(r,\theta,\phi) - \mathbf{B}_{\rm cr}(r,\theta,\phi+\Delta\phi) = -\mathrm{Re}\{\mathrm{grad}\,\Delta V\}$, where ΔV is a spherical harmonic expansion with coefficients $\Delta\gamma_n^m = \gamma_n^m \left(1 - e^{im\Delta\phi}\right)$. Hence by analysing the difference of the magnetic field measured by the two satellites the crustal field coefficients γ_n^m are multiplied with filter factors, and the filter gain is $|\left(1 - e^{im\Delta\phi}\right)| = \sqrt{2(1-\cos m\Delta\phi)}$.

Figure 1 shows the filter gain for three different values of longitudinal separation, $\Delta\phi$, of the satellites. Since *S*warm aims at the determination of the lithospheric field up to spherical harmonic degree and order 133 (spatial scale of 300 km), the optimal longitudinal separation of the lower satellites is about $1.5°$.

A further advantage is that signals from large-scale external contributions that predominantly change in north-south direction are suppressed by the gradient method applied in the east-west direction [*Olsen et al.*, 2004]. Another advantage of using the East-West gradient as opposed to the originally proposed pair of following spacecraft [*Friis-Christensen et al.*, 2002] is that for short time intervals (approximately within 10 seconds), gradients along both neighbouring tracks can still be used.

The magnitude and pattern, of the east-west gradient of a model [*Dyment and Arkani-Hamed*, 1998b] total field anomaly map, ΔF, can be seen in Figure 2. The total field anomaly F at point $\mathbf{r}$, is related to the vector magnetic field $\mathbf{B}$ through $F = \hat{\mathbf{b}} \cdot \mathbf{B}$, where $\hat{\mathbf{b}}$ is the unit vector of the ambient field at $\mathbf{r}(r,\theta,\phi)$.

This model is designed to be a realistic representation of the long wavelength characteristics of the oceanic remanent field. Note that there are five minimums in the gradient map along its southern boundary, as compared to only three minimums in the total field map. This enhanced resolution is accompanied by a decrease in signal magnitude by about a factor of two relative to the total field map. We expect, however, that these gradients should be easily measurable with both our total field and vector instruments. Additional, and complementary, gradient information will be available from the vector magnetic field gradients. This additional information should be especially helpful in deconvolving the lithospheric field signature near the geomagnetic equator, and in determining the orientation of lineated magnetic anomalies [*Parker*, 1997], in addition to its use in characterizing external fields.

2.2 Equivalent source dipole formulation

It is useful to be able to express the measured gradient ΔF in terms of a source function like equivalent source dipoles [*Mayhew*, 1979] for two reasons. First, it allows us to reduce data collected at different altitudes to a common altitude. Second, it provides some insight into the lateral variation of magnetization. The magnetic field $\mathbf{B}(\mathbf{r})$ at a location $\mathbf{r}(r,\theta,\phi)$ caused by a magnetic point dipole $\mathbf{M}(M_{r_1}, M_{\theta_1}, M_{\phi_1})$ at a location $\mathbf{r_1}(r_1,\theta_1,\phi_1)$ can be shown [*Dyment and Arkani-Hamed*, 1998a; *Von Frese et al.*, 1998] to be

$$
\begin{aligned}
\mathrm{B}_r &= \tfrac{-1}{R^3}\left[\left(\tfrac{3AA_1}{R^2}+\cos\delta\right)\mathrm{M}_{r_1}+\left(\tfrac{3AB_1}{R^2}-\tfrac{B_1}{r}\right)\mathrm{M}_{\theta_1}\right.\\
&\qquad\left.+\left(\tfrac{3AC_1}{R^2}-\tfrac{C_1}{r}\right)\mathrm{M}_{\phi_1}\right],\\
\mathrm{B}_\theta &= \tfrac{-1}{R^3}\left[\left(\tfrac{3BA_1}{R^2}-\tfrac{B}{r_1}\right)\mathrm{M}_{r_1}+\left(\tfrac{3BB_1}{R^2}+D\right)\mathrm{M}_{\theta_1}\right.\\
&\qquad\left.+\left(\tfrac{3BC_1}{R^2}+E\right)\mathrm{M}_{\phi_1}\right],\\
\mathrm{B}_\phi &= \tfrac{-1}{R^3}\left[\left(\tfrac{3CA_1}{R^2}-\tfrac{C}{r_1}\right)\mathrm{M}_{r_1}+\left(\tfrac{3CB_1}{R^2}-F\right)\mathrm{M}_{\theta_1}\right.\\
&\qquad\left.+\left(\tfrac{3CC_1}{R^2}+G\right)\mathrm{M}_{\phi_1}\right],
\end{aligned}
$$

where δ is the angle between $\mathbf{r}$ and $\mathbf{r_1}$ and the other symbols are defined as

$$
\begin{aligned}
R &= (r^2+r_1^2-2rr_1\cos\delta)^{1/2},\\
\cos\delta &= \cos\theta\cos\theta_1+\sin\theta\sin\theta_1\cos(\phi-\phi_1),\\
A &= r-r_1\cos\delta,\\
B &= r_1\left(\sin\theta\cos\theta_1-\cos\theta\sin\theta_1\cos(\phi-\phi_1)\right),\\
C &= r_1\sin\theta_1\sin(\phi-\phi_1)\\
D &= \sin\theta\sin\theta_1+\cos\theta\cos\theta_1\cos(\phi-\phi_1),\\
E &= \cos\theta\sin(\phi-\phi_1),\\
F &= \cos\theta_1\sin(\phi-\phi_1),\\
\mathrm{G} &= \cos(\phi-\phi_1).\\
A_1 &= r_1-r\cos\delta,\\
B_1 &= r\left(\cos\theta\sin\theta_1-\sin\theta\cos\theta_1\cos(\phi-\phi_1)\right)\\
\text{and } \mathrm{C}_1 &= -r\sin\theta\sin(\phi-\phi_1).
\end{aligned}
$$

Then $\Delta F = ((\hat{\mathbf{b_a}}\cdot\mathbf{B_a})-(\hat{\mathbf{b_b}}\cdot\mathbf{B_b}))/R_{ab}$, where the a subscript indicates a measurement by the first satellite, a b subscript one by the second satellite and R_{ab} is the distance between the two satellites.

2.3 Gradient observations from the present mini-constellation

In an attempt to better understand the advantages and limitations of gradient measurements, we have reviewed the Ørsted, SAC-C, and CHAMP missions for close encounters. Between mid-2001 and mid-2004, in excess of $33,000$ close encounters

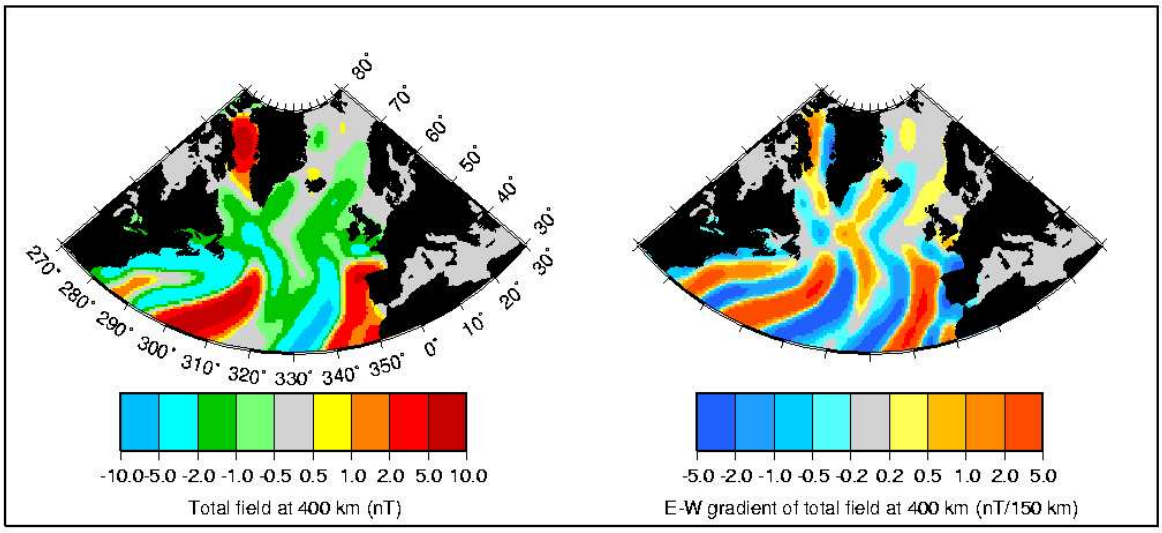

Fig. 2. A comparison of a map of the E-W gradient of the total field with the total field map for the same area. A separation of $1.5°$ is used in the E-W gradient calculation.

were identified between CHAMP and Ørsted, and in excess of $16,000$ were identified between CHAMP and SAC-C. Close encounters are here defined as times when the subsatellite points are within 2° of one another. Because of the orbital geometry, about 60% of the close encounters were in either the northern or southern polar caps. The encounter data, and associated information, can be found at http://planetary-mag.net/close_encounters. Figure 3 and Table 1 summarize close encounters of CHAMP with the SAC-C and Ørsted satellites poleward of 60° North. SAC-C data have been calibrated (see http://www.dsri.dk/ lastec/SAC-C_SHM_Calibration.html for details) using this same close encounter data. Hence we expect that the offsets (Table 1) between SAC-C and CHAMP will be small, as they are. We have selected the data using criteria [*Mandea and Purucker*, 2005] typical for polar regions (night time data from magnetically quiet times) and have imposed the additional constraint that along-track gradients be small and consistent with a crustal source. This close encounter data is similar to that expected from *Swarm* in that it represents observations when the sub-satellite points are within 1.5° of one another at the same time. We did not have to specify a minimum distance because the altitude of the spacecraft differ by about 300 km, ensuring the presence of an adequate gradient. This data differs from that expected from *Swarm* in that the gradients are dominantly vertical instead of horizontal. The horizontal gradients measured between Ørsted and SAC-C are collected from too high an altitude to contain a measurable crustal field gradient. In addition, the close encounter data is made up of mostly total field data, whereas *Swarm* will also have vector field measurements. Figure 3, and accompanying Table 1, show that the lithospheric signal over the north polar cap is reliably isolated by the selection criteria, with about 20% of the data retained. It also demonstrates that the selection criteria are necessary for the isolation of the lithospheric signal. There is a tendency for the predictions to underestimate the observed field, as shown by the slopes, which average about 2. This is especially notable over stronger anomalies. These gradients have evidently captured unmodeled, probably higher frequency, signal. Comparing the gradient measurement with the field measurement, we see a notable improvment in both the correlation coefficient and the offset, with the correlation coefficient improving from about 0.7 to in excess of 0.8. The field model [*Sabaka et al.*, 2004] used to reduce the observations utilized input data through 2002 in creating the model, so we might expect some improvement if we used a field model that incorporated more recent data. However, using a field model such as 07a-05 (Olsen, personal communication), made using data through 2005, does not significantly alter the conclusion. Ørsted and SAC-C are almost equally effective in capturing the gradient, as indicated by the correlation coefficient of 0.84 between the CHAMP-Ørsted observation and model, and the correlation coefficient of 0.83 between the CHAMP-SAC-C observation and model. We also examined close encounters in the southern polar cap (Table 2) and at mid-latitudes (Table 3). Unfortunately, these close encounters did not pass over a signficant number of large anomalies, as revealed by the 'Min Max' range column in the tables. This number captures the minimum and maximum predicted model gradient. Notice that while the range (the difference between the Min and Max) is large for the north polar cap, it is significantly smaller for the south polar cap and the mid-latitude region. So although we can see the same trends and patterns in the south polar and mid-latitude data, the correlation coefficients are nowhere near as good as in the northern polar cap.

3. Conclusion

This study validates the *Swarm* concept of utilizing gradient data to isolate unmodeled, higher frequency, components of the lithospheric magnetic field. The gradient data is also shown to be superior to field data in isolating the lithospheric signal.

Acknowledgments. We thank the Ørsted and CHAMP data centers and project teams for their support. Nils Olsen and Richard Smith are acknowledged for collaborations on many of the developments discussed here. This effort is part of NASA and GFZ contributions to the ESA-led *Swarm* project. We wish to acknowledge the encouragement of Roger Haagmans and John LaBrecque. MEP is supported under NASA contract NAS5-00181. We acknowledge the efforts of two anonymous reviewers to improve the manuscript.

4. References

Dyment, J., and J. Arkani-Hamed, Equivalent source dipoles revisited, *Geophys. Res. Lett.*, *25*, 2003–2006, 1998a.

Dyment, J., and J. Arkani-Hamed, Contribution of lithospheric remanent magnetization to satellite magnetic anomalies over the world's oceans, *J. Geophys. Res.*, *103*, 15,423–15,442, 1998b.

ESA, Gravity Field and Steady-State Ocean Circulation Mission: Report for mission selection, *ESA SP-1233(1)*, ESA Publications Division, ESTEC, Noordwijk, The Netherlands, 1999.

Friis-Christensen, E., H. Lühr, and G. Hulot, *Swarm* - a constellation to study the dynamics of the Earth's magnetic field and its interactions with the Earth system, *DSRI Report 1/2002*, Danish Space Research Institute, Copenhagen, 2002.

Harrison, C., and J. Southam, Magnetic field gradients and their uses in the study of of the earth's magnetic field, *J. Geomagn. Geoelectr.*, *43*, 585–599, 1991.

Hood, P., and D. Teskey, Aeromagnetic gradiometer program of the Geological Survey of Canada, *Geophysics*, *54*, 1012–1022, 1989.

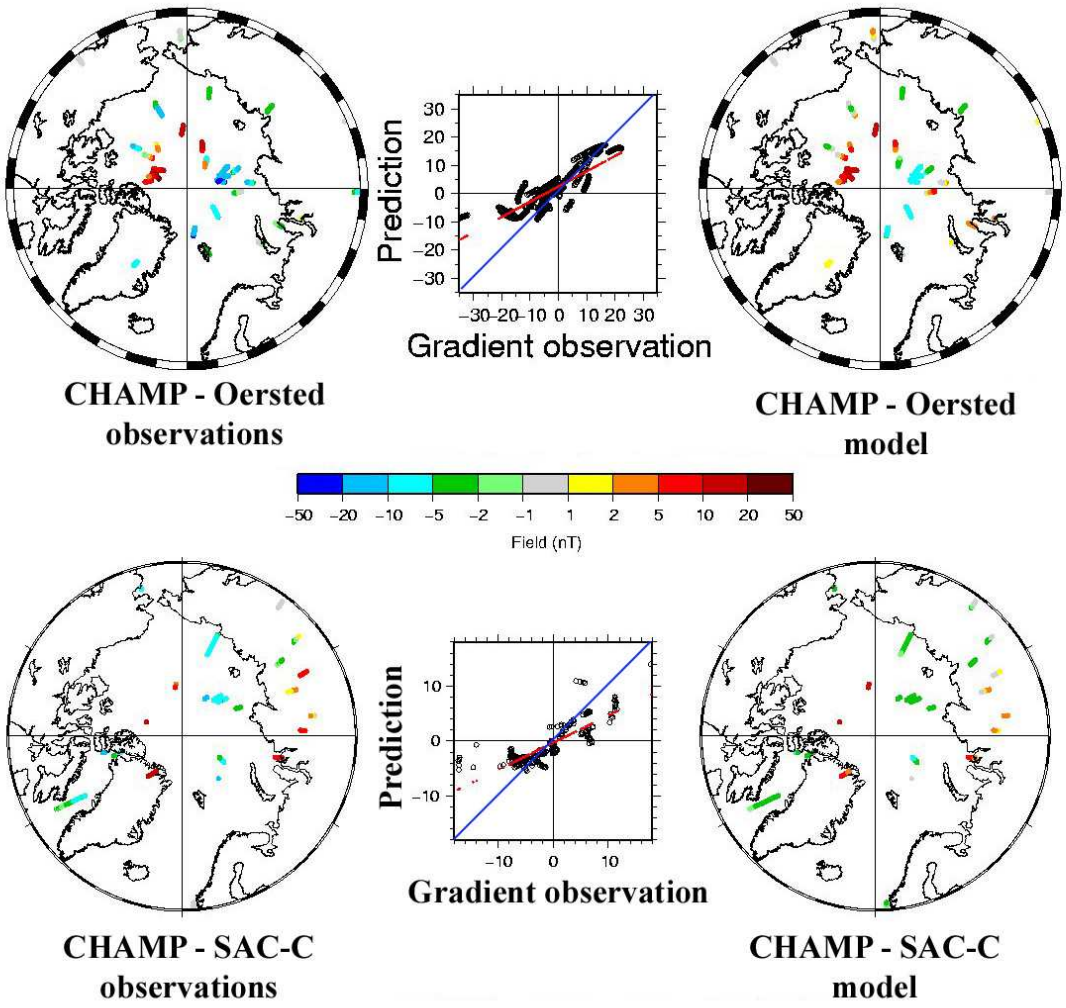

Fig. 3. Observed (left columns) and predicted total field gradient (right columns) during close encounters of Ørsted and CHAMP (top row) and SAC-C and CHAMP (bottom row). The circles locate observation points where the two satellites had sub-satellite locations within 1.5° of one another at the same instant in time, and are color coded with the gradient information. The center column shows the observed vs. predicted gradient (black), a linear least-squares fit (red), and a line with a slope of 1 (blue). The correlation coefficients are in excess of 0.8 for both sets of gradients, and the slopes are close to 2. The observations are night-time data from magnetically quiet times ($Kp < 1^+$ for the present time period, $Kp < 2^0$ for the previous time period) with along-track gradients that are consistent with a crustal source (< 0.3 nT between adjacent observations). The satellites are separated by about 300 km in altitude, with CHAMP being lower. The observed field gradients are shown after removal of either a CM-4 or 07a-05 model field. The predicted field gradients are static degrees 14-65 from the CM-4.

Mandea, M., and M. Purucker, Observing, modeling, and interpreting magnetic fields of the solid earth, *Surveys in Geophysics*, 2005.

Mayhew, M., Inversion of satellite magnetic anomaly data, *J. Geophys.*, *45*, 119–128, 1979.

Olsen, N., et al., *Swarm* - End-to-End mission performance simulator study, ESA contract No 17263/03/NL/CB, *DSRI Report 1/2004*, Danish Space Research Institute, Copenhagen, 2004.

Parker, R., Coherence of signals from magnetometers on parallel paths, *J. Geophys. Res.*, *102*, 5111–5117, 1997.

Sabaka, T. J., N. Olsen, and M. Purucker, Extending comprehensive models of the Earth's magnetic field with Ørsted and CHAMP data, *Geophys. J. Int.*, *159*, 521–547, doi: 10.1111/j.1365–246X.2004.02,421.x, 2004.

Von Frese, R., W. Hinze, and L. Braile, Correction to "spherical earth gravity and magnetic anomaly analysis by equivalent point source inversion", *Earth and Plan. Sci. Lett.*, *163*, 409–411, 1998.

Michael.Purucker (e-mail: purucker@geomag.gsfc.nasa.gov)